Extended Abstracts of the 2006 International Conference on Solid State Devices and Materials, Yokohama, 2006, pp. 462-463

P-2-1

Formation of Mesoporous Pure Silica Zeolite Film

T. Seo[1], T. Yoshino[2], N. Hata[2] and T. Kikkawa[1,2]

[1]Research Center for Nanodevices and Systems, Hiroshima University
Phone: +81-082-424-6265, Fax: +81-082-422-7185,
E-mail: seo@sxsys.hiroshima-u.ac.jp, kikkawa@sxsys.hiroshima-u.ac.jp
[2]MIRAI, Advanced Semiconductor Research Center (ASRC), National Institute of Advanced Industrial Science and Technology (AIST), Tsukuba, 305-8569, Japan

1. Introduction

According to the interconnect scaling rule for silicon ultra-large scale integrated circuits (ULSI), signal delay time increases with decreasing interconnect feature sizes due to increase of interconnect resistance and parasitic capacitance. In order to overcome this problem, low-dielectric-constant (low-k) interlayer dielectric film is needed. However, mechanical strength of the low-k film decreases when pores are formed in interlayer dielectrics. The mechanical strength of zeolite is higher than silica because it has an original structure of three dimensionals network. Zeolite has low-dielectric-constant because it has micropores in the silica skeleton [1]. In this paper, we formed pure silica zeolite and studied the characteristics.

2. Experimental

The MEL type zeolite is in Fig. 1. TBAOH (tetra-butyl ammonium hydroxide), TEOS (tetraethyl orthosilicate), EtOH (ethyl alcohol) and DI water were mixed, heated in autoclave for 110 hours at 100℃ to make precursor. The precursor returned it to the room temperature, and it is heated for ten hours at 100℃ [2,3]. The suspension prepared by this hydrothermal crystallization method contains zeolite crystal. TBAOH was pre-purified by filtering with the ion exchange resin, and TEOS and EtOH used the semiconductor grades. After butanol and surfactant $(EO)_{13}(PO)_{20}(EO)_{13}$ were added to the suspension, the film was formed by spin coating on a Si wafer and calcined in air atmosphere at 400℃.

The aluminum electrode was deposited by using stencil by forming mask to measure electrical characteristics, and metal-insulator-semiconductor (MIS). The measurement was carried out after baking two hours by nitrogen atmosphere at 300℃.

3. Results and Discussion

Fig. 2 is a result of Fourier transform infrared spectroscopy (FT-IR) of the zeolite film. The peak of the zeolite crystal is confirmed about 550cm^{-1} in all samples. This peak show asymmetric stretching mode in five-membered ring blocks in MEL-type zeolite crystal [4]. Moreover, addition of DI water 25wt% enhanced the zeolite formation. After hexamethyldisilazane (HMDS) treatment, the intensity of Si-OH band at 3745cm^{-1}, decreased.

Fig. 3 is atomic force microscope (AFM) micrographs of pure silica zeolite MEL films. The surface roughness increased with water concentration as shown in Fig. 4.

Pore size distribution calculated from the X-ray small angle scattering is shown in Fig. 5. A zeolite crystal could not be confirmed. The higher the water concentration is, the larger average pore sizes are. The average pore size has increased from 4.3 to 7.2.

Water concentration dependency of refractive index and porosity are plotted in Fig. 6. The porosity was calculated by using Lorentz-Lorenz's expression from the refractive index. The porosity increased and the refractive index decreased as the water concentration increased because average pore size increased.

Results of electrical measurements of each sample are plotted in Fig. 7. Leakage current of 25 wt% of water concentration was not able to be measured before HMDS treatment has been introduced. Leakage current and k-value increased as the water concentration increased, and decreased after HMDS treatment.

Fig. 8 is temperature dependency of Leakage current vesus electric field. J_S is expressed in Shottky emission (SE) model as

$$J_S = A^* T^2 \exp\left(\beta_S \sqrt{E} - q\phi_S\right)/k_B T \ , \qquad (1)$$

where A^* is the Richardson constant, q is the electric charge, k_B is the Boltzman constant, β_S is $\sqrt{q^3/4\pi\varepsilon_o\varepsilon_r}$. The slope of SE is $\beta_S/k_B T$, and the slope of Pool-Frenkel (PF) is $\beta_F/k_B T$. Arrhenius plot of $\ln(J/T^2)$ is shown is Fig. 9 for different water contents. Therefore, the conduction for zeolite follows SE model rather than PF model from slope of Fig. 9. Moreover, the Schottky barrier height ϕ_S becomes smaller by an increase of the zeolite component, resalting in the increase of the leakage current.

4. Conclusion

The MEL type pure silica zeolite thin film was formed by the hydrothermal crystallization method, and the existence of the zeolite was confirmed by FT-IR and AFM. The zeolite component increased as adding DI water. Leakage current of the mesoporous pure silica zeolite film was found to be a Schottky current and the Schottky barrier height becomes smaller with increasing the zeolite component, resulting in the increase of the leakage current.

Acknowledgements

This work was supported by NEDO.

References

[1] Z. Wang, H. Wang, A. Mitra, L. Huang, and Y. Yan: Adv. Mater. 13 (2001) 746.
[2] T. Yoshino, G. Guan, N. Hata, N. Fujii, T. Kikkawa: Ext. Abs. SSDM 2005, p. 58.
[3] Z. Wang, Y Yan: Oriented zeolite MFI monolayer films on metal substrates by in situ crystallization.
[4] J. Dong, J. Zou, and Y. Long: Microporous and Mesoporous Materials 57 (2003) 9.

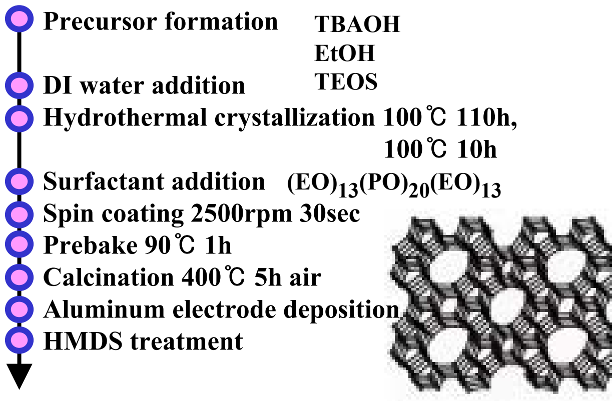

Fig.1. Process flow and schematic diagram of MEL type zeolite structure view from <100> direction.

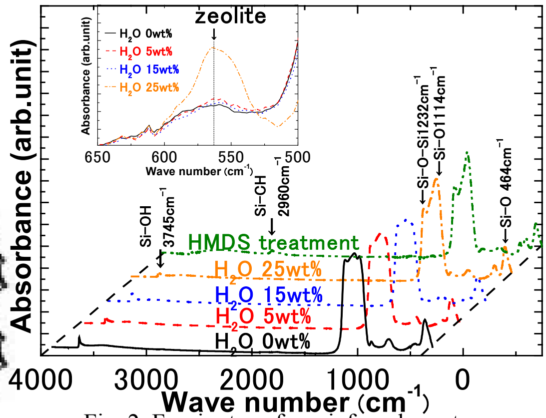

Fig. 2. Fourier transform infrared spectra.

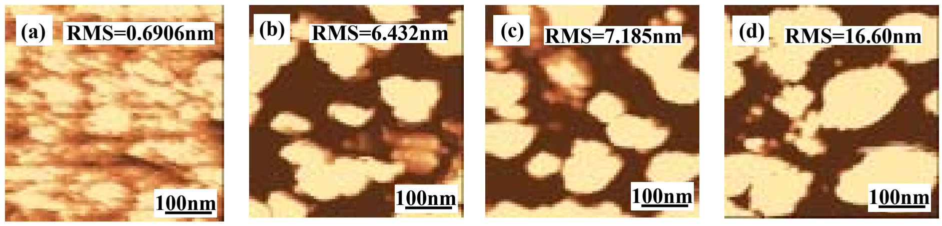

Fig.3. Dependence of water contents on surface morphology of zeolite fimls. (a) DI water 0%, (b) DI water 5%, (c) DI water 15%, (d) DI water 25%

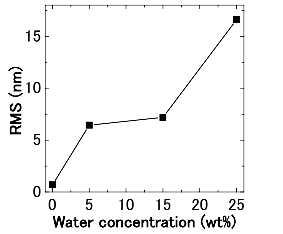

Fig.4. Surface roughness versus water concentration.

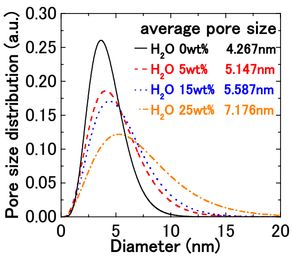

Fig. 5. Dependence of water concentration on pore size distribution measured by small angle x-ray scattering.

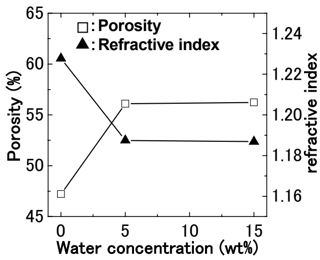

Fig. 6. Water concentration dependency of refractive index and porosity measured by spectroscopic ellipsometry.

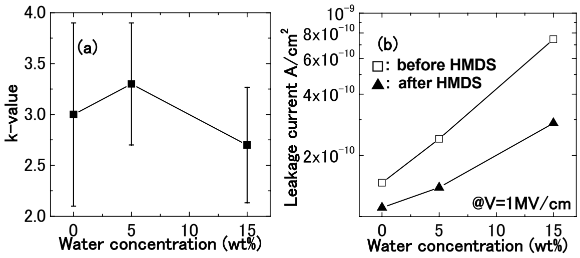

Fig.7. Dependence of water concentration (a) k-value. (b) Leakage current.

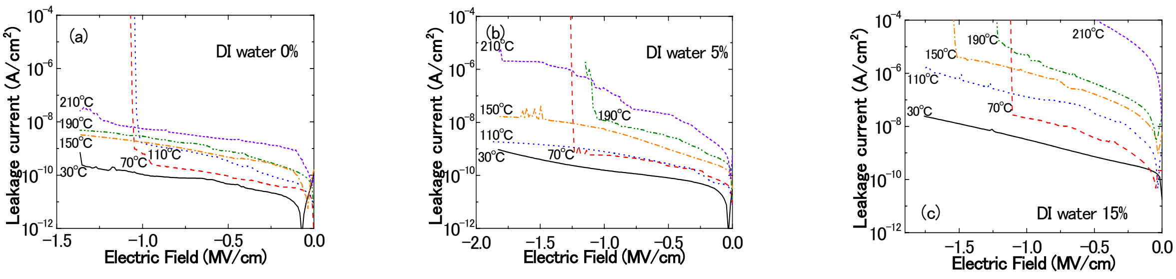

Fig.8. Temperature dependence of Leakage current versus electric field. (a) DI water 0%. (b) DI water 5%. (c) DI water 15%.

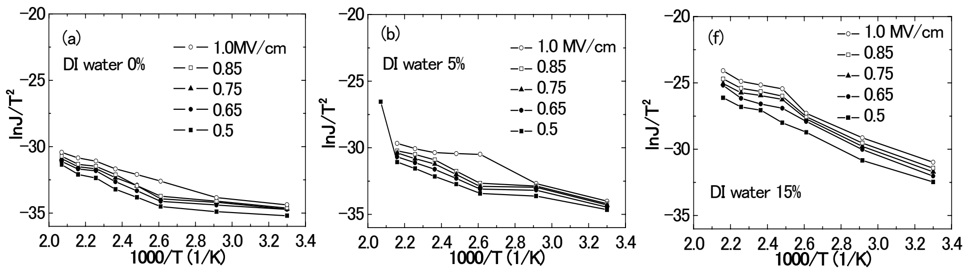

Fig.9. Arrhenius plot of Schottky leakage current. (a) DI water 0%. (b) DI water 5%. (c) DI water 15%.

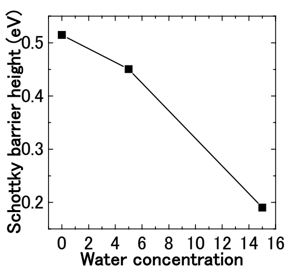

Fig.10. Dependence of Schottky barrier height on water concentration